# The effect of shear deformations' rotary inertia on the vibrating response of multi-physic composite beam-like actuators

Mohammad Malikan[1], Victor A. Eremeyev[1,2*]

[1] Department of Mechanics of Materials and Structures, Faculty of Civil and Environmental Engineering, Gdańsk University of Technology, 80-233 Gdańsk, Poland,

mohammad.malikan@pg.edu.pl, victor.eremeev@pg.edu.pl

[2] DICAAR, Università degli Studi di Cagliari, Via Marengo, 2, 09123, Cagliari, Italy,

victor.eremeev@unica.it

*Corresponding author

## Abstract

In consecutive studies on flexomagneticity (FM), this work investigates the flexomagnetic reaction of a vibrating squared multi-physic beam in finite dimensions. It is assumed that the bending and shear deformations cause rotary inertia. In the standard type of the Timoshenko beam the rotary inertia originated from shear deformations has been typically omitted. It means the rotary inertia resulting from shear deformation is a new concept considered here. Thus, the novelty in this work is that the effect of shear deformation's rotary inertia (SDRI) on the FM response will be considered in detail. When it comes to nanosize, the well-posed nonlocal elasticity assumption of Eringen can be worth choosing. In this study, the weak form of strain-driven nonlocal theory, which means differential form, is taken into hand for easiness. The procedure of solution will be in regard to the advantage of the Galerkin weighted residual technique based on an analytical flow for the meta beam located at simply-simply ends. Verifications of the

mathematical model and solving steps come through macro and nanobeams concerning reputable literature. In pursuit of this step, several separate studies will show how SDRI and FM can influence each other. The observations give some new achievements in the series of studies on FM. It has been earned that the SDRI can directly impress the flexomagnetic feature of small-scale actuators.

**Keywords**: Flexomagneticity; Vibration study; Multi-physic beam; Rotary inertia; Nonlocal elasticity

**Nomenclature:**

$\sigma_{xx}$ : Axial stress

$\tau_{xz}$ : Shear stress

$\varepsilon_{xx}$ : Axial strain

$\gamma_{xz}$ : Shear strain component

$C_{11}$ : Elastic modulus

$q_{31}$ : Component of the third-order piezomagnetic tensor

$H_z$ : Component of the magnetic field

$\xi_{xxz}$ : Component of the higher-order hyper-stress tensor

$g_{31}$ : Influence of the sixth-order gradient elasticity tensor

$a_{33}$ : Component of the second-order magnetic permeability tensor

$\eta_{xxz}$ : Gradient of the axial elastic strain

$f_{31}$ : Component of the fourth-order flexomagnetic coefficients tensor

$B_z$ : Magnetic flux in the $z$ direction

$u_i$ ($i$=1,3): Displacement in the $x$- and $z$- directions

$z$: Thickness coordinate

$u$ and $w$: Mid-plane's axial and lateral displacements

$\phi$ : Rotation of beam elements around the $y$-axis

$P$ : Works performed by external forces

$U$ : Strain energy

$K$ : Kinetic energy

$t$: Time

$\rho$: Material density

$N_x^0$ : Axial in-plane force

$N_x$ : Axial stress resultant

$Q_x$ : Shear stress resultant

$M_x$ : Moment stress resultant

$T_{xxz}$ : Hyper stress resultant

$k_s$ : Shear correction factor

$\Psi$ : Magnetic potential function

$\psi$ : External magnetic potential

$Z_m$ : Residue of the equations

$m_0$, $m_1$, and $m_2$ : Mass moments of inertia

$\mu(nm)^2 = (e_0 a)^2$ : Nonlocal parameter

## 1. Introduction

Due to the individual size effect, magnetic nanoparticles (MNP) have different mechanical, magnetic, and chemical properties compared to micro and macro MNP materials. Therefore, magnetic nanostructures are of great biological, medical, and engineering importance. In addition, magnetic nanoparticles have many applications in several industries, such as the oil industry, including targeted adsorption, remote sensing, transmission, and local heating. For these specific applications, the dispersion and stability of magnetic nanoparticles in suspensions are of great significance [1, 2].

Among magnetic nanostructured materials, metal oxide nanoparticles have an indispensable position due to their exceptional optical, magnetic, and electrical properties. The essential applications of metal oxide nanoparticles have been in a wide range from

biotechnology to various industries. Magnetic nanostructures are a type of metal oxide that can be used through an external magnetic field, and one can employ their properties. Due to the widespread use of magnetic nanoparticles in biomedicine, electronics, catalysts, and other areas, extensive studies have been conducted on various factors affecting their properties [3-6].

The magnetic properties of nanomaterials depend on the physical structure (size and shape of the particles), the softness and flexibility, and the chemical phase of the particles. Magnetic nanoparticles are made from a wide range of magnetic materials. Due to their cheapness, good biocompatibility, proper magnetic dipole moment, and high stability, iron oxide and its related compounds are widely used compared to other metal bases of nanoparticles. It is also the most magnetic natural mineral on Earth. Another most helpful feature of nanoscale iron oxide is its hyper paramagnetic behavior. This property has created a variety of applications for it, such as magnetic resonance imaging, targeted drug delivery, cancer treatment, biosensors, optical applications, data storage, and chemical applications [7-11].

Piezomagnetic materials release the strain created by the deformation as a magnetic field. By attaching electrodes to these materials and then connecting them to a magnetic consumer, mechanical energy can be converted to magnetic power and vice versa. This phenomenon known as piezomagneticity occurring in a few ferrimagnetic and antiferromagnetic non-centrosymmetric crystals. It is characterized by a linear relationship between the system's mechanical strain and magnetic polarization. While mechanical deformation releases a magnetic field, this situation is called the direct effect of such magneto-elastic coupling. However, reversely, appearing mechanical deformations by the outer magnetic field is called the converse effect [12-15].

Piezomagneticity is a well-used phenomenon for designing sensors/actuators [16-18]. Howbeit, a more wonderful magneto-elastic coupling effect has already been discovered, called flexomagneticity [19, 20]. This effect is basically a consequence of induced magnetization and strain gradient correlation so that it may be found in any crystals with less limitation. As a whole, the flexomagnetic influence is still a little-known

phenomenon. Inadequate research on this subject is due to more difficulties with flexomagneticity than piezomagneticity. Outstanding strain gradients can be observed on smaller scales. Some carried out researches have endorsed that the flexomagnetic effect can be more important on the nanoscale than a macro one [19, 20].

In recent years, a few number of groundbreaking investigations have been undertaken in the sector of flexomagnetic structures [19-32]. A characteristic relation of the flexomagneticity in piezomagnetic (PM) structures has been presented in the work of Sidhardh and Ray [19]. An external magnetic field has been produced in the attendance of inhomogeneous strain through thickness. The variational concept has been used to derive the corresponding boundary conditions and the governing equations for the magnetic and mechanical variables. These constitutive equations evaluate the magneto-elastic (ME) structural response. The influence of FM on the bending response of a clamped-free PM nanosize beam is then determined by solving these differential equations. The influence of converse and direct flexomagnetic couplings on the ME reaction was also investigated using a variety of magnetic boundary conditions. A model of Euler-Bernoulli FM nanobeam has been examined in [20], which takes into account the impacts of surface elasticity, piezomagneticity, and flexomagneticity. The accompanying magnetic boundary conditions and dominant differential equations were engendered to examine the effects of reverse and direct FM couplings on the mechanical response. Using size-dependent theoretical solutions, the static bending deformations of the clamped, simply supported, and cantilever nanobeams have been determined. The beam has been exposed to concentrated or uniformly distributed loads. They showed that the FM enhances the bending rigidity apart from the boundary conditions. A two-parameter flexomagnetic model in a cantilever beam has been studied using the Timoshenko beam model by [21]. The size effect phenomenon for a piezomagnetic substance has been studied using the strain gradient. The generic governing equations have been obtained using the virtual work's principle. The influence of FM on the Timoshenko piezomagnetic beam was studied by an analytical solution. Compared to the classical Timoshenko beam model, the numerical findings show that the deflections are diminished upon considering FM. When the beam thickness is reduced, the reduction of

deflection will be more severe. Malikan and his colleagues, in a series of publications, have investigated FM in copious conditions and extended the FM studies seriously. In the framework of the Euler-Bernoulli nanobeam, they captured nonlinear frequencies employing a nonlocal strain gradient model [22] for PM-FM nanosize tube structures. On the other hand, the first nonlinear bending analysis of PM-FM nanobeams has been performed by [23]. The earlier studies hired linear bending equations only. In [23], it was obtained that the nonlinear strains are crucial to considering FM. These researches keep going on the linear and nonlinear buckling [24], demonstrating this achievement that FM is more fundamental in a more minor degree of freedom boundary conditions. Malikan and Eremeyev [25] checked FM in a shear deformable PM nanobeam model and revealed that FM has been impressed by shear deformations. Malikan et al. [26], through microscale PM-FM structures, conducted research on the effect of the thermal environment on the stability of the specimen while various temperature distributions have been assumed. [27] inspected FM effect in a two-dimensional PM plate under biaxial compressions for the first time. The attained results exhibited that aspect ratio (ratio of length to width of the plate) can robustly affect FM response. As a preliminary research, ref [28] evaluated FM in functionally graded (FG) PM micro/nanostructures. More visibility of FM has been displayed in some particular FG nanobeams. Lastly, the surface effect as a dominant one on the nanoscale has been studied for a PM-FM nanobeam subjected to nonlinear deflections [29]. The prepared work ensured that the surface effect is efficacious in FM response. The influence of materials' imperfections inside the piezomagnetic-flexomagnetic structures has been discussed by dint of [30]. The imperfection has been assumed in the framework of porous and vacancies. A new scheme of study on flexomagnetic structures has been presented by [31]. The thermo-elastic coupling investigation has been modeled on the way of Lord-Shulman thermal conductivity theorem. The results promised new aspects to the studies of mechanics of multi-physics materials. Through the medium of a new fundamental flexomagnetic characteristic free energy relation, ref [32] based on both nonlocal integral and differential models, presented new findings in the category of meta structures.

The size effect shall be considered while the discussion focuses on the flexomagnetic response. The nanoscale is a finite-size domain promising a wide range of new aspects for mechanical analyses of meta structures. It can be analyzed theoretically in the body of advanced continuum mechanics. Hence, the effect of this minute size can be evaluated using several state-of-the-art elasticity approaches. Potent literature can be easily found on different nanoscale static and dynamic analyses. The nonlocal effect as the major impact at the nanoscale, in accord with the literature, is divided into two forms, stress-driven nonlocal elasticity (SDM) proposed by Romano and Barretta [33] and strain-driven one expressed by Eringen [34]. The approaches such as strain-driven nonlocal elasticity are derived into two categories; the nonlocal differential model (NDM) and the nonlocal integral one (NIM). The first one is an approximation of the second one. What is more, the SDM is a well-posedness nonlocal model recently expanded further by [35-49]. Within this paper, we have employed the NDM of Eringen. In comparison with Eringen's NIM, the NDM is not always in a well-conditioned state. For example, some literature proved that for cantilever nanobeams, there would be some conflicts in the NDM results [50-52]. This meant that for clamped-free nanobeams in the dynamic conditions, the increase in value of the nonlocal coefficient causes increase in the material's stiffness. This is a paradoxical result compared with the other boundary conditions with the same status of the forces and material. Despite that, the NIM obliterates this inconsistency [53]. In addition to this, the SDM model also eliminates the aforesaid contradiction and can be well-dedicated to the mathematical modeling of nanoscale structures [35-49]. Nevertheless, on the use of NDM, in this paper, the simply-supported conditions will be taken into consideration only, which give consistent results based on the above-mentioned nonlocal models. Considering other boundary conditions is out of the scope of this study.

Given that nanobeams are known as one of the main elements in nanostructures and have several applications in the field of nanotechnology, they should be studied in terms of properties and mechanical behavior under different conditions. The purpose of investigating the vibrations of magnetic nanobeams is to evaluate the performance of piezomagnetic/flexomagnetic features in an oscillating state. However, a nanobeam may be consciously or unconsciously exposed to an external magnetic field, and this field will

undoubtedly affect the performance of the nanobeam. Therefore, in this research, the free vibrations of piezo-flexomagnetic meta beams under the effect of external magnetic load are investigated to prevent errors in nanobeam applications and perform a more appropriate design. To investigate the vibration behavior of finite beams, first, using the traditional Timoshenko model the constitutive relations established. Then the modified Timoshenko beam based on adding rotary inertia effect caused by shear deformations supplies new equilibrium equations. All governing equations and boundary conditions have been extracted using Hamilton's principle. The Timoshenko beam is improved by considering the shear deformations' rotary inertia (SDRI), and the results of both beam theories are compared to each other. Cause that the derivation of equations takes into account the geometric effect (von Kármán strain), the final governing equations, which are in the form of magneto-elastic coupling, are also linear. To solve these equations, the weighted residual method has been used. In the results section, first, the results of this paper are validated, and then the magnetic field generated under external load is extracted. In addition, the flexomagnetic response of the beam under the presence of SDRI is also compared with when the SDRI is absent.

## 2. Mathematical modeling

The simply-supported nanobeam has been figured (Fig. 1). The beam has been adjusted in the Cartesian coordinate system where $z$ coordinate has been assumed along with specimen height. Furthermore, the $x$-axis has been located along the model length. In addition, geometry is defined where $h$ is thickness/height for the square cross-section, and $L$ is used for the length. Finally, the restraints and pinned on both sides have been considered rigid, and the beam is deformable only.
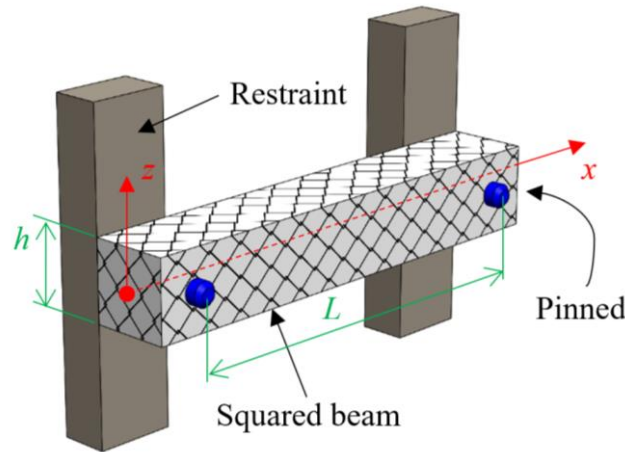
**Fig. 1.** The schematic geometrical shape and physical conditions of the assumed nanobeam

To capture flexomagnetic coupling, there are three well-positioned constitutive magneto-elastic relations illustrated below [19, 20]

$$\sigma_{xx} = C_{11}\varepsilon_{xx} - q_{31}H_z \tag{1}$$

$$\xi_{xxz} = g_{31}\eta_{xxz} - f_{31}H_z \tag{2}$$

$$B_z = a_{33}H_z + q_{31}\varepsilon_{xx} + f_{31}\eta_{xxz} \tag{3}$$

where the appeared components and coefficients are introduced in the nomenclature section.

Vibrations and propagation analyses will be done concerning Timoshenko kinematic field, and the dynamic equilibrium equations will be formulated based on using Eq. 4 [54]

$$\begin{Bmatrix} u_1(x,z,t) \\ u_3(x,z,t) \end{Bmatrix} = \begin{Bmatrix} z\phi(x,t) \\ w(x,t) \end{Bmatrix} \tag{4}$$

The conventional scheme of Lagrangian strain can be found in [32]. So then one can develop Lagrangian strain with respect to Eq. (4) in order to derive the consistent strain relations as shown by Appendix A,

The typical Hamilton's principle enables us to generate constitutive equations,

$$\int_{t_1}^{t_2} (\delta P - \delta U + \delta K) dt = 0 \tag{5}$$

Shortly, when the variational operator ($\delta$ operator) is imposed on a derivative, one obtains $\delta[dy/dx] = d(\delta y)/dx$. This operator plays the primary role to find governing equations. Physically, the total potential energy of a medium has been supposed to variate scantily. Then, the governing equations of deformations of the media have been achieved. The total strain energy of the present nanosystem can be given as,

$$U = \frac{1}{2} \int_V \left( \sigma_{xx}\varepsilon_{xx} + \tau_{xz}\gamma_{xz} + \xi_{xxz}\eta_{xxz} - B_z H_z \right) dV \tag{6}$$

Using kinetic energy, one provides the mass inertia terms as,

$$K = \frac{1}{2} \int_{-h/2}^{h/2} \int_A \rho(z,t) \left( \left( \frac{\partial u_1}{\partial t} \right)^2 + \left( \frac{\partial u_3}{\partial t} \right)^2 \right) dAdz \tag{7}$$

Enforcing the variational technique on Eqs. (6) and (7) induces relations existed in Appendix A as governing equations.

In order to implement the effect of the lateral magnetic field, one uses the below relation defining external work performed by the field,

$$P = \frac{1}{2} \int_0^L N_x^0 \left( \frac{\partial w}{\partial x} \right)^2 dx \tag{8}$$

Afterward, imposing a small variation by using the delta operator on Eq. (8) extends it as available in Appendix A.

To remind that the in-plane compressive force which causes contraction in the magnetic nanobeam is precisely the load mentioned below,

$$N_x^0 = - \int_{-h/2}^{h/2} q_{31} \frac{\Psi}{h} dz \tag{9}$$

Classical and magnetic stress resultants are available in the literature [32] as,

$$\left\{ N_x, M_x, Q_x, T_{xxz} \right\} = \int_{-h/2}^{h/2} \left\{ \sigma_{xx}, \sigma_{xx}z, k_s\tau_{xz}, \xi_{xxz} \right\} dz \tag{10}$$

Note that the value of the shear correction factor has already been calculated for an isotropic macro-structure in some special boundary conditions. Although an exact value of this coefficient has not still been computed for different nonlocal structures, the amount of 5/6 is of use to some extent [55, 56].

As the present mechanical model is one-dimensional, the transverse magnetic field has been assumed as [19, 20]

$$H_z + \frac{\partial \Psi}{\partial z} = 0 \tag{11}$$

Let us deem that the magnetic potential is absent at the bottom of the beam and highest at the top [19, 20],

$$\Psi \begin{Bmatrix} +\dfrac{h}{2} \\ -\dfrac{h}{2} \end{Bmatrix} = \begin{Bmatrix} \psi \\ 0 \end{Bmatrix} \tag{12}$$

Let us combine Eqs. (3), (11), (12), and $\delta U^{Mag}$ relation mentioned in Appendix A, then one can produce the following relations, which are associated with magnetic potential function and vertical magnetic field component,

$$\Psi = \frac{q_{31}}{2a_{33}} \left( z^2 - \frac{h^2}{4} \right) \frac{\partial \phi}{\partial x} + \frac{\psi}{h} \left( z + \frac{h}{2} \right) \tag{13}$$

$$H_z = -z \frac{q_{31}}{a_{33}} \frac{\partial \phi}{\partial x} - \frac{\psi}{h} \tag{14}$$

Subsequently, the governing equations can be developed on the basis of Eqs. (6-8) as,

$$\frac{\partial Q_x}{\partial x} + N_x^0 \frac{\partial^2 w}{\partial x^2} = m_0 \frac{\partial^2 w}{\partial t^2} \tag{15}$$

$$\frac{\partial M_x}{\partial x} + \frac{\partial T_{xxz}}{\partial x} - Q_x = m_1 \frac{\partial^2 \phi}{\partial t^2} \tag{16}$$

This study is the first to implement rotary inertia caused by shear deformations into a piezomagnetic nanobeam. The following equation defines the angle of rotation of the beam containing shear ($\gamma(x,t)$) and bending ($\phi(x,t)$) slopes of the neutral axis as follows [57],

$$\frac{\partial w(x,t)}{\partial x} = \phi(x,t) + \gamma(x,t) \tag{17}$$

The shear deformation causes rotary inertia, which is commonly disappeared in the standard model of the Timoshenko beam. This effect is related to the shear slope of the neutral axis. Indeed, the shear slope is a result of shear deformations.

To include this impact, Eq. (16) shall be modified as,

$$\frac{\partial M_x}{\partial x} + \frac{\partial T_{xxz}}{\partial x} - Q_x = m_1 \frac{\partial^3 w}{\partial x \partial t^2} \tag{18}$$

The expressions of the governing equations can be re-written as,

$$\frac{\partial Q_x}{\partial x} + N_x^0 \frac{\partial^2 w}{\partial x^2} = m_0 \frac{\partial^2 w}{\partial t^2} \tag{19}$$

$$\frac{\partial M_x}{\partial x} + \frac{\partial T_{xxz}}{\partial x} - Q_x = m_1 \frac{\partial^3 w}{\partial x \partial t^2} \tag{20}$$

When the discussion is confined to nanomaterials, a nonlocal effect is inevitable. This nanoscale property can be mathematically shown by the weak form of the nonlocal theorem of Eringen as follows [34],

$$\left(1 - \mu \frac{\partial^2}{\partial x^2}\right) \sigma_{ij} = C_{ijkl} \varepsilon_{ij} \tag{21}$$

in which $\mu (nm)^2 = (e_0 a)^2$ expresses a length scale characteristic which is the so-called nonlocal parameter. Here $e_0$ can be a nonlocal constant whose values are dependent on boundary conditions, nanomaterial structures, and other factors [58]. Moreover, $a$ can be the connection length (e.g., two carbon atoms in the case of carbon nanostructures [59]). The value of the nonlocal coefficient can be varied in the range $0^+ < e_0 a \le 2\ nm$ depending on boundary conditions, molecular arrangements, media dimensions, and other criteria. The relation (21) explains that stress at a point is dependent on the strain at the same point and the neighboring points on a nonlocal media. If we re-write Eq. (21) regarding this definition, it would be $\sigma_{ij} = C_{ijkl} \varepsilon_{ij} + \mu \nabla^2 \left(C_{ijkl} \varepsilon_{ij}\right)$. From a mathematical point of view, the Laplace operator calculates an average of a group of quantities in a region. Thus, the nonlocal stress relation here is divided by strain and the average of strains in the neighborhood. The second one defines the strain dependency on the neighborhood to the main point. In actuality, this differential relation is just a simpler description of the integral model of the nonlocal elasticity of Eringen.

By writing stress and hyper stress components, it gives

$$\left(1 - \mu \frac{\partial^2}{\partial x^2}\right) \xi_{xxz} = \left(g_{31} + \frac{q_{31} f_{31} z}{a_{33}}\right) \frac{\partial \phi}{\partial x} + \frac{f_{31} \psi}{h} \tag{22}$$

$$\left(1 - \mu \frac{\partial^2}{\partial x^2}\right) \sigma_{xx} = z \left(C_{11} + \frac{q_{31}^2}{a_{33}}\right) \frac{\partial \phi}{\partial x} + \frac{q_{31}\psi}{h} \tag{23}$$

$$\left(1 - \mu \frac{\partial^2}{\partial x^2}\right) \tau_{xz} = Gh \left(\phi + \frac{\partial w}{\partial x}\right) \tag{24}$$

One can obtain nonlocal stress and hyper stress resultants by way of Eq. (10) and Eqs. (22-24),

$$\left(1 - \mu \frac{\partial^2}{\partial x^2}\right) T_{xxz} = I_5 \frac{\partial \phi}{\partial x} + I_6 \tag{25}$$

$$\left(1 - \mu \frac{\partial^2}{\partial x^2}\right) M_x = I_2 \frac{\partial \phi}{\partial x} \tag{26}$$

$$\left(1 - \mu \frac{\partial^2}{\partial x^2}\right) Q_x = H_{44} \left(\phi + \frac{\partial w}{\partial x}\right) \tag{27}$$

where the assigned letters are defined as appeared in Appendix B.

Let us unroll Eqs. (26) and (27) by further clarification by dint of Eqs. (19) and (20) as,

$$M_x = -\mu \left(I_5 \frac{\partial^3 \phi}{\partial x^3} + N_x^0 \frac{\partial^2 w}{\partial x^2} - m_0 \frac{\partial^2 w}{\partial t^2} - m_1 \frac{\partial^4 w}{\partial x^2 \partial t^2}\right) + I_2 \frac{\partial \phi}{\partial x} \tag{28}$$

$$Q_x = -\mu \left(N_x^0 \frac{\partial^3 w}{\partial x^3} - m_0 \frac{\partial^3 w}{\partial x \partial t^2}\right) + H_{44} \left(\phi + \frac{\partial w}{\partial x}\right) \tag{29}$$

Now it is possible to expand Eqs. (19) and (20) on the basis of Eqs. (28) and (29) as,

Timoshenko model with neglecting SDRI:

$$\left(1 - \mu \frac{\partial^2}{\partial x^2}\right) \left(N_x^0 \frac{\partial^2 w}{\partial x^2} - m_0 \frac{\partial^2 w}{\partial t^2}\right) + H_{44} \left(\frac{\partial \phi}{\partial x} + \frac{\partial^2 w}{\partial x^2}\right) = 0 \tag{30}$$

$$\left(1 - \mu \frac{\partial^2}{\partial x^2}\right) \left(I_5 \frac{\partial^2 \phi}{\partial x^2} - m_1 \frac{\partial^2 \phi}{\partial t^2}\right) - H_{44} \left(\phi + \frac{\partial w}{\partial x}\right) + I_2 \frac{\partial^2 \phi}{\partial x^2} = 0 \tag{31}$$

Timoshenko model with considering SDRI (Eq. 30 is here the same and was not re-written):

$$\left(1 - \mu \frac{\partial^2}{\partial x^2}\right) \left(I_5 \frac{\partial^2 \phi}{\partial x^2} - m_1 \frac{\partial^3 w}{\partial x \partial t^2}\right) + I_2 \frac{\partial^2 \phi}{\partial x^2} - H_{44} \left(\phi + \frac{\partial w}{\partial x}\right) = 0 \tag{32}$$

Note that the FM parameter did not appear in Eqs. (30-32). The reason is the strain uniformity. If the axial strain is considered a non-uniform distribution, the parameter will

remain in the final equations. However, these equations are still valid for a PFM structure. Also, the results will not be erroneous since the value of the FM coefficient compared to that of the strain gradient parameter ($g_{31}$) is relatively insignificant. In fact, $g_{31}$ is a determinative factor in analyzing flexomagnetic structures. The amount of this quantity is still obscure, and it also may not be a constant value. However, in this paper, the value of the strain gradient factor is considered equal to the crystalline size of the selected material.

Dimensionless parameters provide a more straightforward solution; therefore, one can introduce the terms collected in Appendix B. Thereupon, one can rewrite Eqs. (30-32) as,

1) Piezo-flexomagnetic (PFM) Timoshenko nanobeam with excluding SDRI (TB):

$$N^* \frac{\partial^2 W}{\partial X^2} - \delta^* \frac{\partial^2 W}{\partial \Lambda^2} - \Gamma \left( N^* \frac{\partial^4 W}{\partial X^4} - \delta^* \frac{\partial^4 W}{\partial X^2 \partial \Lambda^2} \right) + H^* \left( \frac{\partial \Phi}{\partial X} + \frac{\partial^2 W}{\partial X^2} \right) = 0 \tag{33}$$

$$g^* \frac{\partial^2 \Phi}{\partial X^2} - M_1^* \frac{\partial^2 \Phi}{\partial \Lambda^2} - \Gamma \left( g^* \frac{\partial^4 \Phi}{\partial X^4} - M_1^* \frac{\partial^4 \Phi}{\partial X^2 \partial \Lambda^2} \right) + D^* \frac{\partial^2 \Phi}{\partial X^2} - H^* \left( \Phi + \frac{\partial W}{\partial X} \right) = 0 \tag{34}$$

2) Piezo-flexomagnetic (PFM) Timoshenko nanobeam with taking SDRI (RI) (Eq. 33 is here the same and was not re-written):

$$g^* \frac{\partial^2 \Phi}{\partial X^2} - M_1^* \frac{\partial^3 W}{\partial X \partial \Lambda^2} - \Gamma \left( g^* \frac{\partial^4 \Phi}{\partial X^4} - M_1^* \frac{\partial^5 W}{\partial X^3 \partial \Lambda^2} \right) + D^* \frac{\partial^2 \Phi}{\partial X^2} - H^* \left( \Phi + \frac{\partial W}{\partial X} \right) = 0 \tag{35}$$

## 3. Solution process

With the understanding of the Galerkin weighted residual process solution, vibrations equations are getting solved depending on simply-supported ends, in this section. This analytical method develops and expresses algebraic equations via determined functions applied for medium's end conditions. And then, in order to report numerical results, the acquired relations have to be solved [28].

There have been two unknown terms in the frequency relations, $W(X)$ and $\Phi(X)$, where the proceeding of the solution will start by introducing the following functions for each of them,

$$\left\{ \begin{array}{c} W(X,\Lambda) \\ \Phi(X,\Lambda) \end{array} \right\} = \sum_{m=1}^{N} \left\{ \begin{array}{c} a_m(X) \\ b_m(X) \end{array} \right\} \exp(i\Omega\Lambda) \qquad (36)$$

where $a_m$ and $b_m$ are corresponded to

$$\left\{ \begin{array}{c} a_m(X) \\ b_m(X) \end{array} \right\} = \int_0^1 \left\{ \begin{array}{c} W_m(X) \\ \Phi_m(X) \end{array} \right\} Z_m(X) dX \qquad (37)$$

To obtain $Z_m$, one must substitute Eq. (36) into the final equations and place the residue in Eq. (37). As mentioned earlier, the simply-supported end conditions (S) have been discussed in this paper. To do this, some well-posed trigonometric functions are utilized as follows,

$$\left\{ \begin{array}{c} W_m(X) \\ \Phi_m(X) \end{array} \right\} = \left\{ \begin{array}{c} \sin(m\pi X) \\ \cos(m\pi X) \end{array} \right\} \qquad (38)$$

We here assume that the functions of Eq. (38) are able to satisfy the simply supported boundary conditions ($W = \Phi = M_X = 0$ at $X = 0,1$).

Fill in Eqs. (33-35) in accord with Eq. (36) yields the equations emerged in Appendix C. How the natural frequency is calculated is also briefly mentioned there.

## 4. Discussion and numerical results

### 4.1. Results accuracy

Here we verify our results and exhibit the accuracy of the formulation and solving method. Firstly, with the help of the robust Abaqus software, Table 1 has been prepared, in which the natural frequency based on Hertz for a macro beam with specifications mentioned at the top of the Table has been calculated. The variable in the Table is the slenderness coefficient, which is the ratio of length to beam's thickness. Assuming a moderately thick beam to a thin beam, the calculations have been completed. A comparison of the results of Abaqus and the present ones clearly shows the good accuracy of the outcomes of the present work. The thinner the beam, the further the accuracy will obtain.

Although by presenting Table 1 the proper precision of the relations and the method of solving the present work can be confirmed to some extent, it is necessary to compare the results for a nanoscale beam. This was achieved by means of authoritative reference [60] and by preparing Table 2. In this part, the dimensionless beam is analyzed with the mentioned properties at the beginning of the Table. Here, too, the calculations of the present work can be realized with reasonable exactness. Moreover, this accuracy may increase as the value of the nonlocal parameter increases. A column is also added to both Tables providing the error percentage of the results based on the subsequent relation,

$$erf\% = \frac{|present - reference|}{reference} \times 100 \qquad (39)$$

**Table 1.** Validation of formulation and solution based on Abaqus for a squared macro beam ($C_{11}$=210e3 MPa, $v$= 0.3, $h$=10 mm, $\rho$=2.2 tonne/mm$^3$, SS)

| | $\omega$ (Hz) | | |
|---|---|---|---|
| $L/h$ | Present | Abaqus | Erf% |
| 10 | 0.86842 | 0.86601 | 0.27828 |
| 12 | 0.60554 | 0.60435 | 0.19690 |
| 14 | 0.44599 | 0.44534 | 0.14595 |
| 16 | 0.34202 | 0.34163 | 0.11415 |
| 18 | 0.27054 | 0.27029 | 0.09249 |
| 20 | 0.21931 | 0.21915 | 0.07300 |
| 22 | 0.18135 | 0.18124 | 0.06069 |
| 24 | 0.15246 | 0.15238 | 0.05250 |
| 26 | 0.12995 | 0.12989 | 0.04619 |
| 28 | 0.11208 | 0.11204 | 0.03570 |
| 30 | 0.09765 | 0.09762 | 0.03073 |
| 32 | 0.08584 | 0.08582 | 0.02330 |
| 34 | 0.07605 | 0.07603 | 0.02630 |
| 36 | 0.06785 | 0.06783 | 0.02948 |
| 38 | 0.06090 | 0.06088 | 0.03285 |
| 40 | 0.05496 | 0.05495 | 0.01819 |

**Table 2.** Validation of formulation and solution for a squared nanobeam ($C_{11}$=10e6, $v$= 0.3, $\rho$=1, $h$=1, SS)

| $L/h$ | $\mu$ | Present | [60] Timoshenko | Erf% |
|---|---|---|---|---|
| 100 | 0.0 | 9.8679 | 9.8683 | 0.0040 |
| | 0.5 | 9.6331 | 9.6335 | 0.0041 |
| | 1.0 | 9.4143 | 9.4147 | 0.0042 |
| | 1.5 | 9.2097 | 9.2101 | 0.0043 |
| | 2.0 | 9.0179 | 9.0183 | 0.0044 |
| | 2.5 | 8.8377 | 8.8380 | 0.0033 |
| | 3.0 | 8.6678 | 8.6682 | 0.0046 |
| | 3.5 | 8.5074 | 8.5077 | 0.0035 |
| | 4.0 | 8.3555 | 8.3558 | 0.0035 |
| | 4.5 | 8.2115 | 8.2118 | 0.0036 |
| | 5.0 | 8.0747 | 8.0750 | 0.0037 |
| | | | | |
| 20 | 0.0 | 9.8281 | 9.8381 | 0.1016 |
| | 0.5 | 9.5942 | 9.6040 | 0.1020 |
| | 1.0 | 9.3763 | 9.3858 | 0.1012 |
| | 1.5 | 9.1726 | 9.1819 | 0.1012 |
| | 2.0 | 8.9816 | 8.9907 | 0.1012 |
| | 2.5 | 8.8020 | 8.8110 | 0.1021 |
| | 3.0 | 8.6328 | 8.6416 | 0.1018 |
| | 3.5 | 8.4730 | 8.4816 | 0.1013 |
| | 4.0 | 8.3218 | 8.3302 | 0.1008 |
| | 4.5 | 8.1784 | 8.1867 | 0.1013 |
| | 5.0 | 8.0421 | 8.0503 | 0.1018 |
| | | | | |
| 10 | 0.0 | 9.7075 | 9.7454 | 0.3889 |
| | 0.5 | 9.4765 | 9.5135 | 0.3889 |
| | 1.0 | 9.2612 | 9.2973 | 0.3882 |
| | 1.5 | 9.0600 | 9.0953 | 0.3881 |
| | 2.0 | 8.8713 | 8.9059 | 0.3885 |
| | 2.5 | 8.6940 | 8.7279 | 0.3884 |
| | 3.0 | 8.5269 | 8.5601 | 0.3878 |
| | 3.5 | 8.3690 | 8.4017 | 0.3892 |
| | 4.0 | 8.2196 | 8.2517 | 0.3890 |
| | 4.5 | 8.0780 | 8.1095 | 0.3884 |

| | | | |
|---|---|---|---|
| 5.0 | 7.9434 | 7.9744 | 0.3887 |

## 4.2. Frequency analysis

This sub-section is prepared to analyze the natural frequency of the nano-actuator assumed in this work. The numerical results will be provided for an actual and physical model to make the present problem realistic. For this aim, according to Table 3 [19, 20, 61], the natural frequencies of the $CoFe_2O_4$ composite nanomaterial have been calculated.

**Table 3.** Properties of the magnetic nanosize structure

| $CoFe_2O_4$ |
|---|
| $C_{11}$=286 GPa, $v$=0.32 |
| $\rho$=4.89 kg/dm$^3$ |
| $q_{31}$=580.3 N/A.m |
| $a_{33}$=1.57×10$^{-4}$ N/A$^2$ |

### 4.2.1 Slenderness ratio

Let us now study the different physical and environmental states of the modeled nanobeam. First of all, let us get started on the study by examining the various values of the vital parameter of the slenderness coefficient. As it is already known, this coefficient is the product of dividing the length by the thickness of the beam, which is valid for macro beams as well as nanobeams. This coefficient indicates the importance of shear deformations. So that the selected value of 5 to 11 can indicate the thick and relatively thick area of the beam. Fig. 2 is investigated for piezomagnetic nanobeams based on the hypothesis that in one case, the beam follows the Timoshenko model (TB), and in the other case, the beam has a rotational inertial effect (RI) due to shear deformations (SDRI). The results are presented for the first frequency mode. The results of the figure show that when the amount of slenderness coefficient is smaller (beam is thicker), the SDRI effect increases. This result makes sense because the thicker the beam, the more urgent the shear deformations. It is noteworthy that the SDRI increases the stiffness of the nanobeam and thus increases its natural frequency.
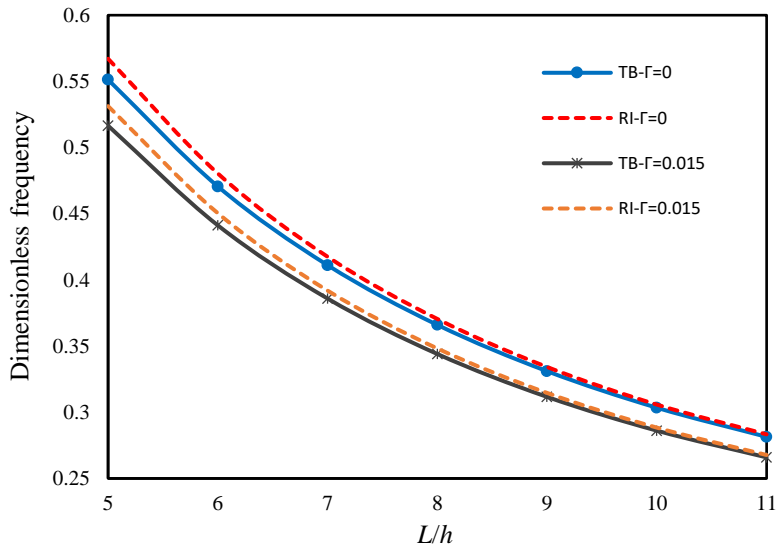
**Fig. 2.** Variations of the dimensionless frequency with slenderness ratio for RI and TB for various nonlocal coefficient values ($N^*$=1e-4, $m$=1, PFM)

### 4.2.2 Nonlocal factor

The importance of investigating the additional small-scale parameter in the mechanical analysis of nanostructures with respect to references has been well-established. Therefore, this study evaluates the effect of different numerical values for this parameter to determine its effect on the analytical model. Fig. 3 shows the location for the local beam using $\Gamma$=0. The maximum value of $\Gamma$ is also selected to be 0.015. Four cases can be seen in the diagram. Piezo-flexomagnetic nanobeam (PFM) in RI and TB modes and piezomagnetic nanobeam in the two mentioned cases. There is no flexomagnetic effect in piezomagnetic nanobeams (PM). As it turns out, the nonlocal parameter has a decreasing effect on the beam frequency while using the SS case. A closer look at the figure suggests that the flexomagnetic effect will be more significant at higher values of the nonlocal parameter. In fact, the results for PFM small scale beams will go slightly away from those of PM in larger values of $\Gamma$.
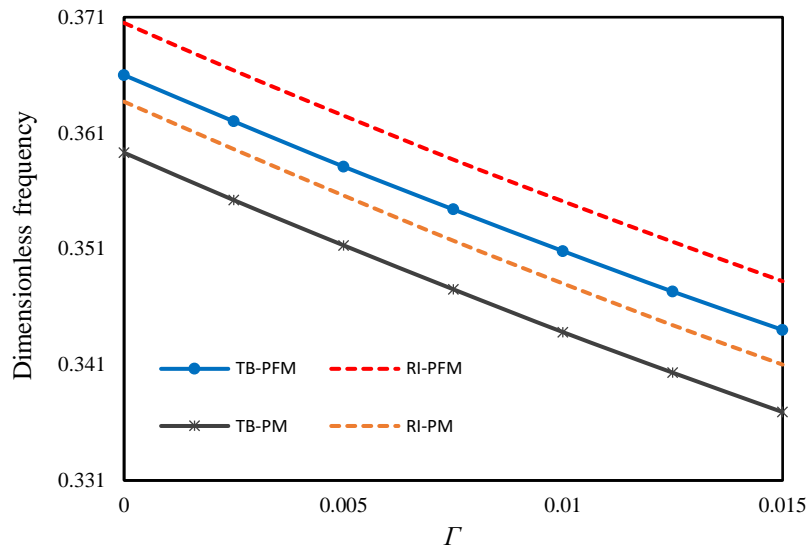
**Fig. 3.** Influence of flexomagneticity on dimensionless frequency versus nonlocal parameter for RI and TB (*L/h*=8, *N\**=1e-4, *m*=1)
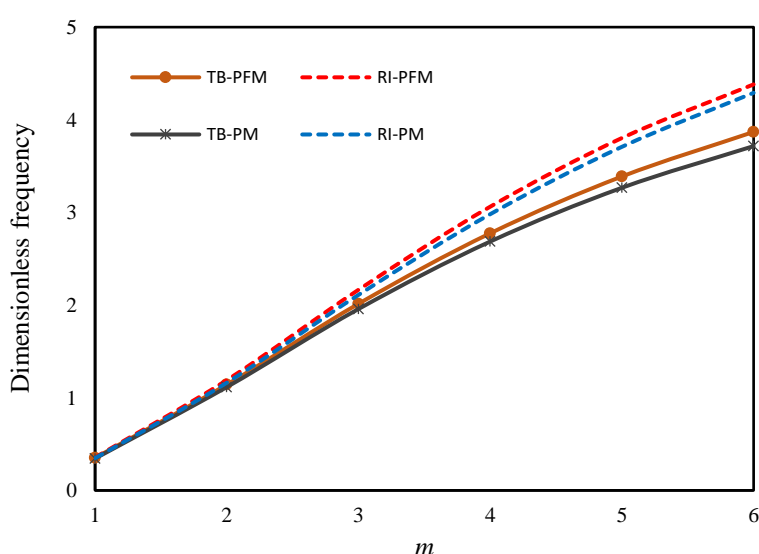
### 4.2.3 Frequency mode number

Drawing a series of diagrams 4 to 7 enables us to thoroughly investigate the effect of frequency modes on the behavior of magnetic nanobeams in the two cases; the standard Timoshenko beam and the modified Timoshenko beam including SDRI. All four figures are drawn for frequency modes 1 to 6. Fig. 4 represents the results in four nanobeams cases. Piezo-flexomagnetic nanobeams with SDRI (PFM-RI) and without it (PFM-TB) and then piezomagnetic nanobeams with SDRI (PM-RI) and without it (PM-TB). The first result that can be obtained is that the difference between results of PFM nanobeams and those of PM will be more tremendous at higher frequency modes. This means that the effect of flexomagnetic will be more significant in higher frequency modes.

Interestingly, this increase is greater in the TB beam than in the RI beam. In fact, it can be here seen that FM will be affected by SDRI. On the other hand, another conclusion that can be drawn from this figure is that increasing the frequency modes increases the importance of SDRI. This increase occurs further for the PM beam than the PFM beam between the TB and RI cases.

Fig. 5 is a sequel to Fig. 4, indicating the frequency modes in different slenderness coefficients. The foremost apparent achievement of this figure is that in higher frequency modes and thicker beams, the effect of SDRI will be very significant. However, the difference between TB and RI will be more negligible at larger slenderness ratios. Another consequence of this figure could be that the results curve of the frequency modes will be nonlinear with larger curvature for thicker beams. This is apparent in the case of increase of the mode numbers. However, moving the beam to a relatively thick and thin area, increasing frequency modes involves an almost linear increase in frequency.

Fig. 6 is almost similar to Fig. 5 but with minor differences. In this figure, the larger in-plane force has been chosen. As seen, the results have changed completely. It is here observed that the thinner the beam, the more the natural frequency. However, the important result of the previous figure is still valid, and here, too, the effect of SDRI is greater in the thicker beam.

Finally, Fig. 7 in this section is drawn by not considering the in-plane force and removing this force. The results and behavior of the diagram are very similar to those in Fig. 5. However, the point to consider here is the greater discrepancy between the results of RI and TB beams. Actually, it is possible to deduce that the less the in-plane force, the greater the effect of SDRI.
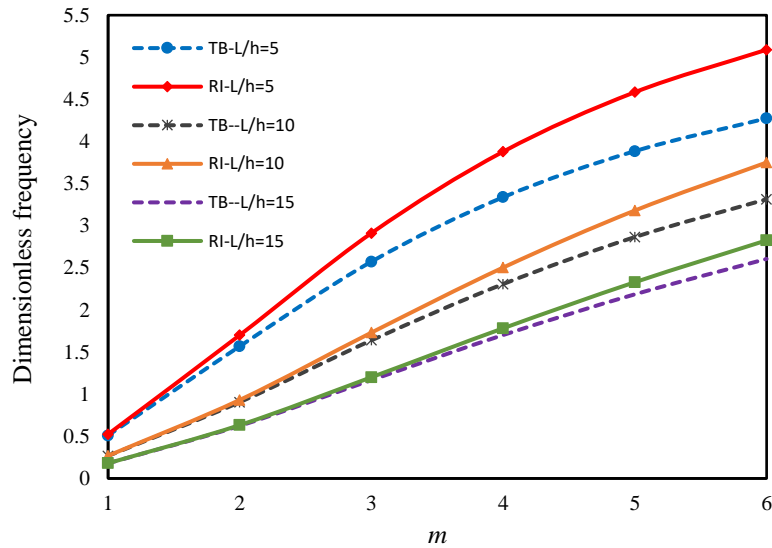
**Fig. 4.** Variations of dimensionless frequency versus mode numbers for various structures (*L*/*h*=8, *N*\*=1e-4, *Γ*=0.01)
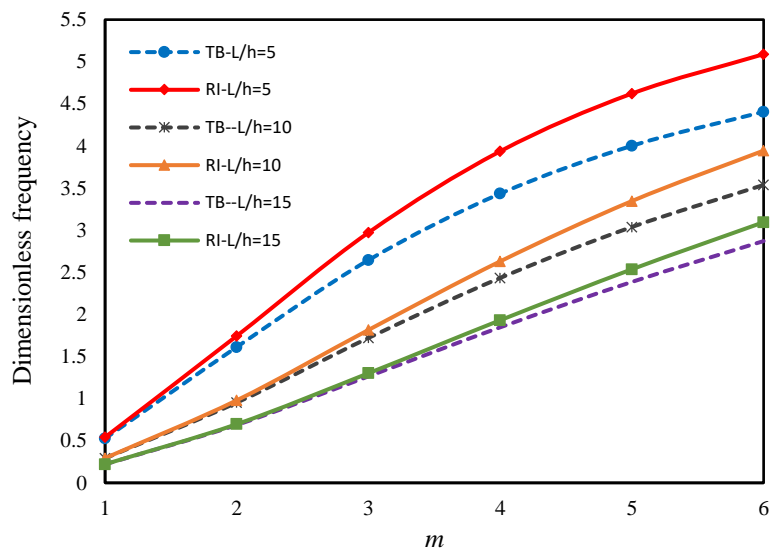


**Fig. 5.** Influence of slenderness ratio on dimensionless frequency in different mode numbers (*N*\*=1e-4, *Γ*=0.01)
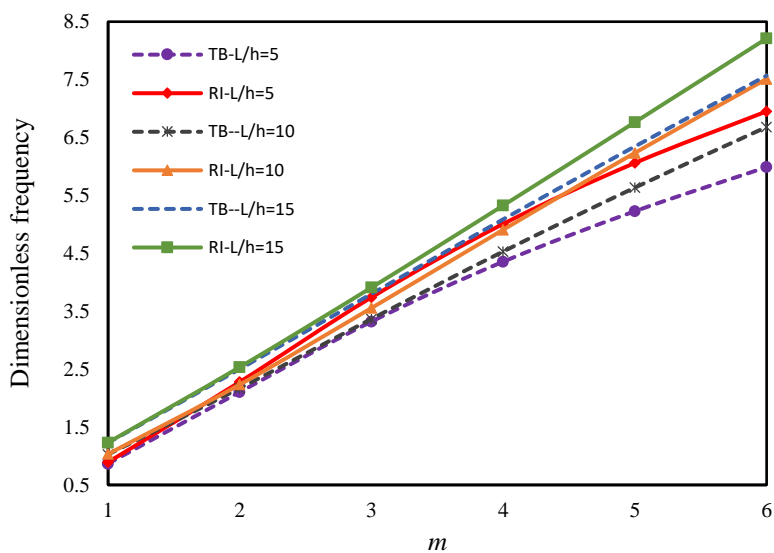


**Fig. 6.** Variations of the dimensionless frequency with mode numbers for different slenderness ratios (*N*\*=1e-2, *Γ*=0.01)

**Fig. 7.** Influence of frequency mode numbers on dimensionless frequency in several slenderness ratios and absence of axial magnetic force ($N^*$=0, $\varGamma$=0.01)

### 4.2.4 In-plane force

The in-plane compressive force resulting from the transverse magnetic field leads to the contraction of the magnetic nanobeam. According to the research background, increasing the amount of this force leads to increasing the material's stiffness. The result is also seen in Fig. 8. In this case, the higher the force values, the higher the natural frequency of the magnetic nanobeam. However, the change of the values of this force does not affect the behavior of ordinary nanobeam (NB), which is quite reasonable. Because ordinary nanobeams do not have magnetic properties and will not naturally react in the magnetic field against the potential of an external magnet.

Moreover, if one pays attention to the numerical values of the graph, two interesting results will be extracted. First, as the in-plane force increases, the PM/PFM beam's results diverge in both TB and RI modes. This means that the in-plane force affected the SDRI. The second result is that as the axial load enlarges, the TB/RI beam's results will be closer in PFM and PM states. This implies that increasing the longitudinal magnetic force reduces the flexomagnetic effect of the material.
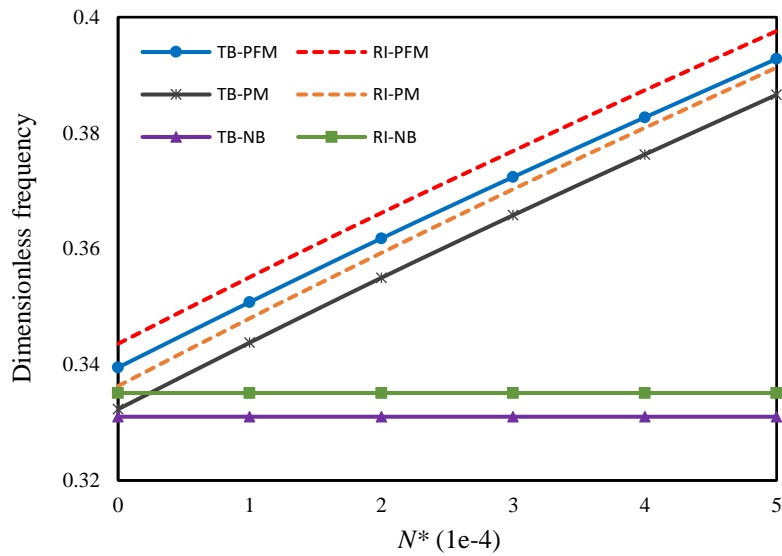
**Fig. 8.** Comparison of the frequency response of different nanostructures by variations of axial magnetic force ($L/h$=8, $m$=1, $\Gamma$=0.01)

## 5. Conclusions

The most intention of this article is to explore and estimate the impact of shear deformation's rotary inertia (SDRI) on the flexomagnetic response of a piezomagnetic actuator. The actuator has been implemented in a small-scale one-dimensional beam framework. A converse magneto-elastic coupling effect has been assessed based on the particular case of magnetic boundary conditions on the beam's transverse topmost and bottommost surfaces. The supposed magnetic field is imposed in line with the lateral dimension of the beam. The beam is theoretically modeled by the common Timoshenko beam approach as well as a modified version of the Timoshenko beam on the basis of SDRI. In the contractual Timoshenko model, the rotary inertia results from bending; however, in the new version, the shear deformation itself generates rotary inertia. Employing these beam models and the nonlocal continuum hypothesis demonstrated characteristics equations for wave propagation and vibrations. And then, utilizing an analytical flow on the basis of the Galerkin weighted residual technique re-derived the constitutive equations in terms of algebraic ones. At long last, in order to compute natural frequencies, the attained algebraic equations will proceed further by a solution step in Matlab. Thereafter, results have been discussed detailedly with respect to various

significant factors influencing the nano actuator's mechanical behavior. The efforts of this research work have indicated the following findings,

- Small-scale evaluation has led to further notable flexomagneticity.

- Higher frequency modes give a more prominent flexomagnetic response.

- The SDRI affects the flexomagnetic response of the nanobeam.

- The impact of SDRI has been remarkable while the actuator looks thicker, and the situation is for higher frequency modes.

- The in-plane load originating from the magnetic field affects the SDRI, and the smaller values of this force bring SDRI further practical.

## Appendix A:

Strain and hyper strain fields:

$$\varepsilon_{xx} = z\frac{\partial \phi}{\partial x}$$

$$\gamma_{xz} = \phi + \frac{\partial w}{\partial x}$$

$$\eta_{xxz} = \frac{\partial \varepsilon_{xx}}{\partial z} = \frac{\partial \phi}{\partial x}$$

Governing equations:

$$\delta U_1^{Mech} = -\int_0^L \left( \frac{\partial Q_x}{\partial x}\delta w - Q_x \delta\varphi + \frac{\partial M_x}{\partial x}\delta\varphi + \frac{\partial T_{xxz}}{\partial x}\delta\varphi \right) dx$$

$$\delta U_1^{Mag} = -\int_0^L \int_{-h/2}^{h/2} \frac{\partial B_z}{\partial z}\delta\Psi dz dx$$

$$\delta U_2^{Mech} = \left( Q_x \delta w + M_x \delta\varphi + T_{xxz}\delta\varphi \right)\Big|_0^L$$

$$\delta U_2^{Mag} = \int_0^L \left( B_z \delta\Psi \right)\Big|_{-h/2}^{h/2} dx$$

$$\delta K = \rho \int\limits_{-h/2}^{h/2} z^2 dz \times \int\limits_0^L \left( \frac{\partial \phi}{\partial t} \frac{\partial \delta \phi}{\partial t} \right) dx + \rho \int\limits_{-h/2}^{h/2} dz \times \int\limits_0^L \left( \frac{\partial w}{\partial t} \frac{\partial \delta w}{\partial t} \right) dx = 0$$

$$\delta P = \int\limits_0^L \left( N_x^0 \frac{\partial \delta w}{\partial x} \frac{\partial w}{\partial x} \right) dx$$

where index 2 is used to show boundary conditions relations, and index 1 is dedicated to denoting governing equations.

## Appendix B:

Material inherent parameters:

$$I_2 = \left( C_{11} + \frac{q_{31}^2}{a_{33}} \right) \int\limits_{-h/2}^{h/2} z^2 dz, \ I_4 = \int\limits_{-h/2}^{h/2} \frac{\psi q_{31}}{h} dz, \ I_5 = \int\limits_{-h/2}^{h/2} g_{31} dz,$$

$$I_6 = \int\limits_{-h/2}^{h/2} \frac{\psi f_{31}}{h} dz, \ H_{44} = k_s \int\limits_{-h/2}^{h/2} G dz, \ \{m_0, m_1\} = \rho \int\limits_{-h/2}^{h/2} \{1, z^2\} dz,$$

Dimensionless parameters:

$$W = \frac{w}{L}, \ \Phi = \phi, \ \Gamma = \frac{\mu}{L^2}, \ X = \frac{x}{L}, \ M_0^* = \frac{m_0}{\rho L}, \ M_1^* = \frac{m_1}{\rho L^3}, \ N^* = \frac{N^{Mag}}{C_{11}L}, \ \delta^* = \frac{h}{L},$$

$$H^* = \frac{H_{44}}{C_{11}L}, \ \Lambda = \frac{t\xi}{L}, \ \Omega = \frac{\omega L}{\xi}, \ D^* = \frac{I_2}{C_{11}L^3}, \ \xi = \sqrt{\frac{C_{11}}{\rho}}, \ g^* = \frac{I_5}{C_{11}L^3},$$

## Appendix C:

AC-1:
$$\begin{bmatrix} -\Gamma\left(N^* m^4 \pi^4 - \delta^* \Omega^2 m^2 \pi^2\right) & -H^* m\pi \\ -H^* m^2 \pi^2 - N^* m^2 \pi^2 + \delta^* \Omega^2 & \\ & M_1^* \Omega^2 - \Gamma\left(g^* m^4 \pi^4 + M_1^* \Omega^2 m^2 \pi^2\right) \\ -H^* m\pi & +D^* m^2 \pi^2 - g^* m^2 \pi^2 - H^* \end{bmatrix} \begin{Bmatrix} a_m \\ b_m \end{Bmatrix} = 0$$

AC-2:
$$\begin{bmatrix} \delta^* \Omega^2 - \Gamma\left(N^* m^4 \pi^4 - \delta^* \Omega^2 m^2 \pi^2\right) & -H^* m\pi \\ -H^* m^2 \pi^2 - N^* m^2 \pi^2 & \\ & -g^* m^2 \pi^2 - \Gamma g^* m^4 \pi^4 \\ M_1^* \Omega^2 m\pi + M_1^* \Omega^2 m^3 \pi^3 - H^* m\pi & -D^* m^2 \pi^2 - H^* \end{bmatrix} \begin{Bmatrix} a_m \\ b_m \end{Bmatrix} = 0$$

The determinant of the coefficients matrices illustrated by AC-1&2 simply render polynomial algebraic equations whose solutions grant the dimensionless natural frequencies. These polynomial equations are derived respectively with a few efforts as,

AC-3: $\Omega^4 + \dfrac{\alpha_2}{\alpha_1}\Omega^2 + \dfrac{\alpha_3}{\alpha_1} = 0$

where

$$\alpha_1 = \Gamma\delta^* M_1^* - \Gamma^2\delta^* M_1^* m^2\pi^2 + N^* H^* \dfrac{\delta^* M_1^*}{m^2\pi^2} - \delta^*\Gamma M_1^*$$

$$\alpha_2 = M_1^*\Gamma N^* m^2\pi^2 + \Gamma^2 N^* M_1^* m^4\pi^4 - \Gamma^2\delta^* g^* m^4\pi^4 + \Gamma\delta^* D^* m^2\pi^2 - \Gamma\delta^* g^* m^2\pi^2 - \Gamma\delta^* H^*$$

$$-N^* M_1^* + \delta^* D^* + N^*\Gamma M_1^* m^2\pi^2 - H^* M_1^* - \delta^*\Gamma g^* m^2\pi^2 + H^*\Gamma M_1^* m^2\pi^2 - \delta^* g^* - \dfrac{\delta^* H^*}{m^2\pi^2}$$

$$\alpha_3 = \Gamma^2 N^* m^6\pi^6 g^* - \Gamma N^* D^* m^4\pi^4 + \Gamma N^* g^* m^4\pi^4 + \Gamma N^* H^* m^2\pi^2 + H^*\Gamma g^* m^4\pi^4 - H^* D^* m^2\pi^2$$

$$+H^* m^2\pi^2 g^* + H^{*2} + N^*\Gamma g^* m^4\pi^4 - N^* D^* m^2\pi^2 + N^* m^2\pi^2 g^* - H^{*2}$$

AC-4: $\Omega^2 + \dfrac{\lambda_2}{\lambda_1} = 0$

where

$$\lambda_1 = -\delta^* g^* - \delta^*\Gamma g^* m^2\pi^2 - \delta^* D^* - \dfrac{\delta^* H^*}{m^2\pi^2} - \delta^* g^* m^2\pi^2 + M_1^* H^* - \delta^*\Gamma g^* m^4\pi^4 - \delta^* D^* m^2\pi^2$$

$$-\delta^* H^* + M_1^* H^* m^2\pi^2$$

$$\lambda_2 = \Gamma N^* g^* m^4\pi^4 + \Gamma^2 N^* g^* m^6\pi^6 + \Gamma N^* D^* m^4\pi^4 + \Gamma N^* H^* m^2\pi^2 - H^* m^2\pi^2 g^* - H^*\Gamma g^* m^4\pi^4$$

$$-H^* D^* m^2\pi^2 - H^{*2} - N^* g^* m^2\pi^2 - N^*\Gamma g^* m^4\pi^4 - N^* D^* m^2\pi^2 - N^* H^* + H^{*2}$$

The solutions of AC-3&4 are performed with the Matlab package leading to natural frequencies.

## References

[1] I. Obaidat, I. Bashar, Y. Haik, Magnetic properties of magnetic nanoparticles for efficient hyperthermia, Nanomaterials 5 (2015) 63-89.

[2] P. C. Morais, Photoacoustic spectroscopy as a key technique in the investigation of nanosized magnetic particles for drug delivery systems, Journal of Alloys and Compounds 483 (2009) 544-548.

[3] G. Simonsen, M. Strand, G. Øye, Potential applications of magnetic nanoparticles within separation in the petroleum industry, Journal of Petroleum Science and Engineering 165 (2018) 488-495.

[4] V. Reddy, N. P. Annapu, Pathak, R. Nath, Particle size dependent magnetic properties and phase transitions in multiferroic BiFeO3 nano-particles, Journal of Alloys and Compounds 543 (2012) 206-212.

[5] Á. Ríos, M. Zougagh, Recent advances in magnetic nanomaterials for improving analytical processes, Trends in Analytical Chemistry 84 (2016) 72-83.

[6] D. Lisjaka, A. Mertelj, Anisotropic magneticnano: A review of their properties, syntheses and potential application, Progress in Materials Science 95 (2018) 286-328.

[7] A.V.B. Reddy, Z. Yusop, J. Jaafar, Y. V. M. Reddy, A. B. Aris, Z. A. Majid, J. Talib, G. Madhavi, Recent progress on Fe-based nanoparticles: Synthesis, properties, characterization and environmental applications, Journal of Environmental Chemical Engineering 4 (2016) 3537–3553.

[8] Y. Wei, B. Han, X. Hu, Y. Lin, X. Wang, X. Deng, Synthesis of Fe3O4 nanoparticles and their magnetic properties, Chinese Materials Conference 2 (2012) 632-637.

[9] S. Ebrahimisadr, B. Aslibeiki, R. Asadi, Magnetic hyperthermia properties of iron oxide nanoparticles: The effect of concentration, Physica C: Superconductivity and its applications 549 (2018) 119-121.

[10] L. L.-P. Diandra, R. D. Rieke, Magnetic properties of nanostructured materials, Chemistry of materials 8 (1996) 1770-1783.

[11] C. Fei, Y. Zhang, Z. Yang, Y. Liu, R. Xiong, J. Shi, X. Ruan, Synthesis and magnetic properties of hard magnetic (CoFe2O4)–soft magnetic (Fe3O4) nano-composite ceramics by SPS technology, Journal of Magnetism and Magnetic Materials 323 (2011) 1811-1816.

[12] A. F. Kabychenkov, F. V. Lisovskii, Flexomagnetic and flexoantiferromagnetic effects in centrosymmetric antiferromagnetic materials, Technical Physics 64 (2019) 980-983.

[13] E. A. Eliseev, A. N. Morozovska, M. D. Glinchuk, R. Blinc, Spontaneous flexoelectric/flexomagnetic effect in nanoferroics, Physical Review B 79 (2009) 165433.

[14] P. Lukashev, R. F. Sabirianov, Flexomagnetic effect in frustrated triangular magnetic structures, Physical Review B 82 (2010) 094417.

[15] P. Zubko, G. Catalan, A. Buckley, P. R. L. Welche, J. F. Scott, Strain-gradient-induced polarization in SrTiO3 single crystals, Physical Review Letters 99 (2007) 167601.

[16] R. Gholami, R. Ansari, A unified nonlocal nonlinear higher-order shear deformable plate model for postbuckling analysis of piezoelectric-piezomagnetic rectangular nanoplates with various edge supports, Composite Structures 166 (2017) 202-218.

[17] A. M. Zenkour, M. Arefi, N. A. Alshehri, Size-dependent analysis of a sandwich curved nanobeam integrated with piezomagnetic face-sheets, Results in Physics 7 (2017) 2172-2182.

[18] M. Malikan, M. Krasheninnikov, V. A. Eremeyev, Torsional stability capacity of a nano-composite shell based on a nonlocal strain gradient shell model under a three-dimensional magnetic field, International Journal of Engineering Science 148 (2020) 103210.

[19] S. Sidhardh, M. C. Ray, Flexomagnetic response of nanostructures, Journal of Applied Physics 124 (2018) 244101.

[20] N. Zhang, Sh. Zheng, D. Chen, Size-dependent static bending of flexomagnetic nanobeams, Journal of Applied Physics 126 (2019) 223901.

[21] J. Sladek, V. Sladek, M. Xu, et al. A cantilever beam analysis with flexomagnetic effect, Meccanica 56 (2021) 2281–2292.

[22] M. Malikan, V. A. Eremeyev, On the geometrically nonlinear vibration of a piezo-flexomagnetic nanotube, Mathematical Methods in the Applied Sciences, (2020). https://doi.org/10.1002/mma.6758

[23] M. Malikan, V. A. Eremeyev, On Nonlinear Bending Study of a Piezo-Flexomagnetic Nanobeam Based on an Analytical-Numerical Solution, Nanomaterials 10 (2020) 1762.

[24] M. Malikan, N. S. Uglov, V. A. Eremeyev, On instabilities and post-buckling of piezomagnetic and flexomagnetic nanostructures, International Journal of Engineering Science 157 (2020) 10339.

[25] Malikan, M., Eremeyev, V.A. Flexomagneticity in buckled shear deformable hard-magnetic soft structures, Continuum Mechanics and Thermodynamics 34 (2022) 1-16.

[26] M. Malikan, T. Wiczenbach, V. A. Eremeyev, On thermal stability of piezo-flexomagnetic microbeams considering different temperature distributions, Continuum Mechanics and Thermodynamics 33 (2021) 1281-1297.

[27] M. Malikan, V. A. Eremeyev, Flexomagnetic response of buckled piezomagnetic composite nanoplates, Composite Structures 267 (2021) 113932.

[28] M. Malikan, T. Wiczenbach, V. A. Eremeyev, Thermal buckling of functionally graded piezomagnetic micro- and nanobeams presenting the flexomagnetic effect, Continuum Mechanics and Thermodynamics (2021). https://doi.org/10.1007/s00161-021-01038-8

[29] M. Malikan, V. A. Eremeyev, Effect of surface on the flexomagnetic response of ferroic composite nanostructures; nonlinear bending analysis, Composite Structures 271 (2021) 114179.

[30] M. Malikan, V. A. Eremeyev, K. K. Żur, Effect of Axial Porosities on Flexomagnetic Response of In-Plane Compressed Piezomagnetic Nanobeams, Symmetry 12 (2020) 1935.

[31] M. Malikan, V. A. Eremeyev, On dynamic modeling of piezomagnetic/flexomagnetic microstructures based on Lord–Shulman thermoelastic model, Archive of Applied Mechanics, (2022). https://doi.org/10.1007/s00419-022-02149-7

[32] M. Malikan, V. A. Eremeyev, On a flexomagnetic behavior of composite structures, International Journal of Engineering Science 175 (2022) 103671.

[33] G. Romano, R. Barretta, Stress-driven versus strain-driven nonlocal integral model for elastic nano-beams, Composites Part B: Engineering 114 (2017) 184-188.

[34] A. C. Eringen, Nonlocal continuum field theories, Springer, New York, (2002).

[35] R. Penna, L. Feo, A. Fortunato, R. Luciano, Nonlinear free vibrations analysis of geometrically imperfect FG nano-beams based on stress-driven nonlocal elasticity with initial pretension force, Composite Structures 255 (2021) 112856.

[36] M. Sara Vaccaro, F. Paolo Pinnola, F. Marotti de Sciarra, R. Barretta, Limit behaviour of Eringen's two-phase elastic beams, European Journal of Mechanics - A/Solids 89 (2021) 104315.

[37] M. S. Vaccaro, F. Marotti de Sciarra, R. Barretta, On the regularity of curvature fields in stress-driven nonlocal elastic beams, Acta Mechanica 232 (2021) 2595–2603.

[38] M. S. Vaccaro, F. P. Pinnola, F. Marotti de Sciarra, R. Barretta, Dynamics of Stress-Driven Two-Phase Elastic Beams, Nanomaterials 11 (2021) 1138.

[39] F. Paolo Pinnola, M. Sara Vaccaro, R. Barretta, F. Marotti de Sciarra, Finite element method for stress-driven nonlocal beams, Engineering Analysis with Boundary Elements 134 (2022) 22-34.

[40] A. Francesco Russillo, G. Failla, G. Alotta, F. Marotti de Sciarra, R. Barretta, On the dynamics of nano-frames, International Journal of Engineering Science 160 (2021) 103433.

[41] M. S. Vaccaro, F. P. Pinnola, F. Marotti de Sciarra, R. Barretta, Elastostatics of Bernoulli–Euler Beams Resting on Displacement-Driven Nonlocal Foundation, Nanomaterials 11 (2021) 573.

[42] R. Barretta, M. Čanađija, F. Marotti de Sciarra, A. Skoblar, R. Žigulić, Dynamic behavior of nanobeams under axial loads: Integral elasticity modeling and size-dependent eigenfrequencies assessment, Mathematical Methods in the Applied Sciences (2021). https://doi.org/10.1002/mma.7152

[43] R. Barretta, F. Marotti de Sciarra, M. Sara Vaccaro, On nonlocal mechanics of curved elastic beams, International Journal of Engineering Science 144 (2019) 103140.

[44] R. Barretta, F. Fabbrocino, R. Luciano, F. Marotti de Sciarra, G. Ruta, Buckling loads of nano-beams in stress-driven nonlocal elasticity, Mechanics of Advanced Materials and Structures 27 (2020) 869-875.

[45] A. Apuzzo, R. Barretta, F. Fabbrocino, S. A. Faghidian, R. Luciano, F. Marotti de Sciarra, Axial and torsional free vibrations of elastic nano-beams by stress-driven two-phase elasticity, Journal of Applied and Computational Mechanics 5 (2019) 402-413.

[46] R. Barretta, L. Feo, R. Luciano, Some closed-form solutions of functionally graded beams undergoing nonuniform torsion, Composite Structures 123 (2015) 132-136.

[47] R. Barretta, R. Luciano, F. Marotti de Sciarra, A fully gradient model for euler-bernoulli nanobeams, Mathematical Problems in Engineering 2015 (2015) 495095.

[48] R. Barretta, S. A. Fazelzadeh, L. Feo, E. Ghavanloo, R. Luciano, Nonlocal inflected nano-beams: A stress-driven approach of bi-Helmholtz type, Composite Structures 200 (2018) 239-245.

[49] A. Apuzzo, R. Barretta, S. A. Faghidian, R. Luciano, F. Marotti de Sciarra, Nonlocal strain gradient exact solutions for functionally graded inflected nano-beams, Composites Part B: Engineering 164 (2019) 667-674.

[50] K. G. Eptaimeros, C. Chr. Koutsoumaris, G. J. Tsamasphyros, Nonlocal integral approach to the dynamical response of nanobeams, International Journal of Mechanical Sciences 115–116 (2016) 68-80.

[51] J. Fernández-Sáez, R. Zaera, J.A. Loya, J.N. Reddy, Bending of Euler–Bernoulli beams using Eringen's integral formulation: A paradox resolved, International Journal of Engineering Science 99 (2016) 107-116.

[52] R. Barretta, F. Marotti de Sciarra, Analogies between nonlocal and local Bernoulli–Euler nanobeams, Archive of Applied Mechanics 85 (2015) 89-99.

[53] M. Faraji Oskouie, R. Ansari, H. Rouhi, A numerical study on the buckling and vibration of nanobeams based on the strain and stress-driven nonlocal integral models, International Journal of Computational Materials Science and Engineering 07 (2018) 1850016.

[54] J. N. Reddy, Nonlocal nonlinear formulations for bending of classical and shear deformation theories of beams and plates, International Journal of Engineering Science 48 (2010) 1507-1518.

[55] G. Romano, A. Barretta, R. Barretta, On torsion and shear of Saint-Venant beams, European Journal of Mechanics - A/Solids 35 (2012) 47-60.

[56] P. Madabhusi-Raman, J. F. Davalos, Static shear correction factor for laminated rectangular beams, Composites: Part B 27 (1996) 285-293.

[57] H. Yu, X. Chen, P. Li, Analytical Solution for Vibrations of a Modified Timoshenko Beam on Visco-Pasternak Foundation Under Arbitrary Excitations, International Journal of Structural Stability and Dynamics (2021). https://doi.org/10.1142/S0219455422500456.

[58] A. C. Eringen, D. G. B. Edelen, On nonlocal elasticity, International Journal of Engineering Science 10 (1972) 233–248.

[59] S. Narendar, S. Gopalakrishnan, Scale effects on buckling analysis of orthotropic nanoplates based on nonlocal twovariable refined plate theory, Acta Mechanica 223 (2012) 395–413.

[60] J. N. Reddy, Nonlocal theories for bending, buckling and vibration of beams, International Journal of Engineering Science 45 (2007) 288-307.

[61] A. B. Rajput, S. Hazra, N. Nath Ghosh, Synthesis and characterisation of pure singlephase CoFe2O4 nanopowder via a simple aqueous solution-based EDTA-precursor route, Journal of Experimental Nanoscience 8 (2013) 629–39.